

RSC Advances



This is an *Accepted Manuscript*, which has been through the Royal Society of Chemistry peer review process and has been accepted for publication.

Accepted Manuscripts are published online shortly after acceptance, before technical editing, formatting and proof reading. Using this free service, authors can make their results available to the community, in citable form, before we publish the edited article. This *Accepted Manuscript* will be replaced by the edited, formatted and paginated article as soon as this is available.

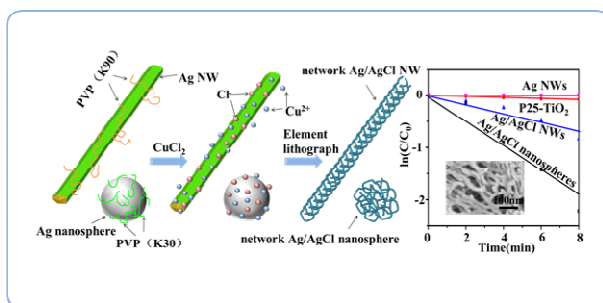
You can find more information about *Accepted Manuscripts* in the [Information for Authors](#).

Please note that technical editing may introduce minor changes to the text and/or graphics, which may alter content. The journal's standard [Terms & Conditions](#) and the [Ethical guidelines](#) still apply. In no event shall the Royal Society of Chemistry be held responsible for any errors or omissions in this *Accepted Manuscript* or any consequences arising from the use of any information it contains.

5

Graphical Abstract

Ag/AgCl network-structures exhibit high photocatalytic performance for the selective-degradation of 4-CP under UV-light, suggesting potential application for organic pollutant elimination.



A Special Ag/AgCl Network-nanostructure for Selective Catalytic Degradation of Refractory Chlorophenol Contaminants†

Cite this: DOI: 10.1039/x0xx00000x

Zaidi Huang^a, Ming Wen^{*a,b}, Dandan Wu^a and Qingsheng Wu^{*a}

Received 00th January 2012,
Accepted 00th January 2012

DOI: 10.1039/x0xx00000x

www.rsc.org/

A special Ag/AgCl network-nanostructure was synthesized based on Ag nanowire (NW) or nanosphere template through the element lithographic network construction process. The structure of obtained Ag/AgCl is 3D nanoscale network-structure that consists of the network NWs with the average diameter of ~ 20 nm and the porous channels with narrow macropore distribution from 50 to 100 nm. As-designed network-nanostructures not only provides firm frame support for the active sites, but also offers large surface areas and lots of reaction performance chambers, and consequently facilitates reactant diffusion and transport greatly. Employed as UV-driven plasmonic photocatalysts, the formulated Ag/AgCl nano-networks exhibit excellent performance and stability for the selective degradation of chlorophenol contaminants. Compared with the commercial P25-TiO₂, the prepared Ag/AgCl network-nanostructures show much higher photocatalytic activity, in which the network-structured nanospheres are better than network-structured nanowires toward the selective degradation of 4-chlorophenol with the reaction rate constant of 0.28 min⁻¹, suggesting the good potential application for organic pollutant elimination.

Introduction

In environmental management, there is a difficult point to degrade the toxic organic contaminants since lots of them are resistant to conventional chemical and biological treatments. The chlorophenol aromatic compounds are a kind of the most refractory pollutants existing in industrial effluents, especially 4-chlorophenol (4-CP), which is carcinogenic, mutagenic, teratogenic, nonbiodegradable and highly toxic. Thus, catalytic degradation as a sustainability approach can reduce the negative impacts on water bodies and benefit to the reuse and regeneration.¹⁻³ Till now, some TiO₂-based catalysts have been developed for the photodegradation of the organic pollutants.⁴⁻¹⁴ However, it is still difficult to fulfil the selective degradation of chlorophenol contaminants. Therefore, the exploration of new catalysts to treat chlorophenol is necessary to undergo.

Nowadays, the metallic nanostructures featured with evident surface plasmon resonance (SPR) have become good candidates for the photodegradation of organic contaminants.^{15,16} Among these plasmonic photocatalysts, Ag/AgCl materials have been focused lots of attention,¹⁷⁻²² because they can exhibit remarkable resonant behaviour when

interacting with ultraviolet (UV) and visible (vis) photons through an excitation of SPR.²³ Up to now, Ag@AgCl nanoparticles (NPs),^{24,25} Ag/AgCl nanocubics,²⁶ and Ag/AgCl-based nanocomposites²⁷ have been investigated for the development of plasmonic photocatalysts and the application to the degradation of organic contaminants. In addition, offering large surface areas, three dimensional (3D) network-structures can not only give excellent performance for the reaction, which is a result of the existence of fertile active sites for catalysis (such as corners, edges, steps, etc).²⁸⁻³² but also facilitate reactant diffusion and transport greatly. However, there is no report about the network-structured Ag/AgCl

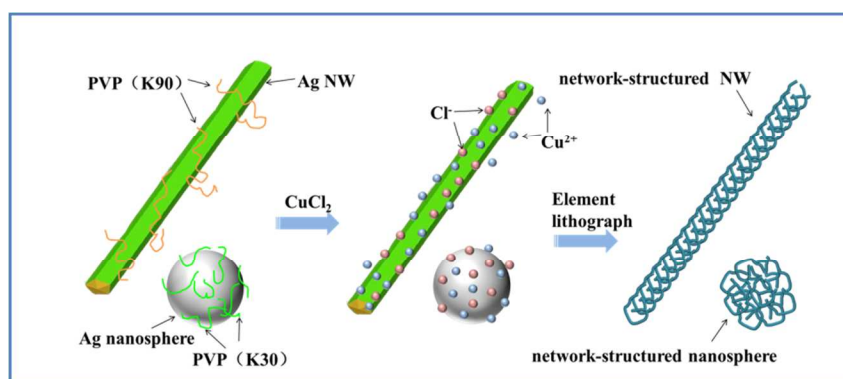


Fig. 1 Schematic view of the procedure for the construction of Ag/AgCl network-nanostructures based on Ag NW and nanosphere via ELNC process.

nanocomposites, and let alone used for the selective-degradation of chlorophenol compounds. Consequently, it remains a great challenge for the launch of efficient route for the synthesis of network-structured Ag/AgCl nanocomposites and employment as plasmonic photocatalysts to selectively degrade refractory chlorophenol contaminants.

In this work, 3D Ag/AgCl network-nanostructures, with the network nanowires (NWs) at the average diameter of ~20nm and the pore channels at narrow macropore distribution from 50 to 100nm, were synthesized based on Ag NWs or nanospheres template through element lithographic network construction (ELNC) process. Used as plasmonic photocatalysts, they could exhibit much higher catalytic performance and better stability for the selective-degradation of 4-CP, compared with commercially available P25-TiO₂ under UV-light irradiation. The formulated Ag/AgCl network-structures can be suggested to well apply in the organic pollutant elimination. The proposal formation mechanism, reaction activity and reusability were investigated in detail in this work.

Results and discussion

Network-structured Ag/AgCl plasmonic photocatalysts were synthesized through the ELNC process based on Ag NWs or nanospheres template. Ag NWs were prepared in an improved ethylene glycol process by employing the so-long-chain PVP (K90, MW=800000) as structure directing agent. The synergistic interaction between the carbonyl groups on long-

chain PVP macromolecule and silver ions results in the one-dimensional (1D) structure. As shown in Fig. 1, based on the template of as-prepared Ag NWs, etching agent of CuCl₂ was introduced into reaction system. Then, AgCl NPs generated on the surface of Ag NWs by the integration between Ag⁺ and Cl⁻. Meanwhile, Cu²⁺ can be attracted to the surface of Ag NWs by electrostatic interaction. Since the standard reduction potentials (SHE) of the Cu²⁺/Cu redox couple is 0.34V, which is higher than that of the AgCl/Ag redox couple (0.22V vs SHE), so some Ag atoms from Ag NWs was oxidized to Ag⁺ by Cu²⁺ (Ag⁺+Cl⁻→AgCl), and generated AgCl coupled with Ag accompanying with the formation of large amount of the porous channels. This ELNC process finally leads to the formation of network-structured Ag/AgCl NWs. Besides having firm frame supporting for the active sites, Ag/AgCl network-structures can offer large surface area and reaction performance chambers, which prefers to facilitate reactant diffusion and transport. If so-long-chain PVP was taken place by short one (K30, MW= 580000), network-structured Ag/AgCl nanospheres can be acquired from Ag nanospheres. The formation process was monitored by field-emission scanning electron microscopy (FESEM), X-ray diffraction (XRD) patterns and energy dispersive X-ray spectroscopy (EDS) analysis (Fig. S1†). In this reaction system, reaction temperature and solvent are important factors for the fabrication of Ag/AgCl network structures (Fig. S2 and S3†). The Ag/AgCl network-nanostructures with well distributed macropores can only be prepared at 170°C in ethylene glycol.

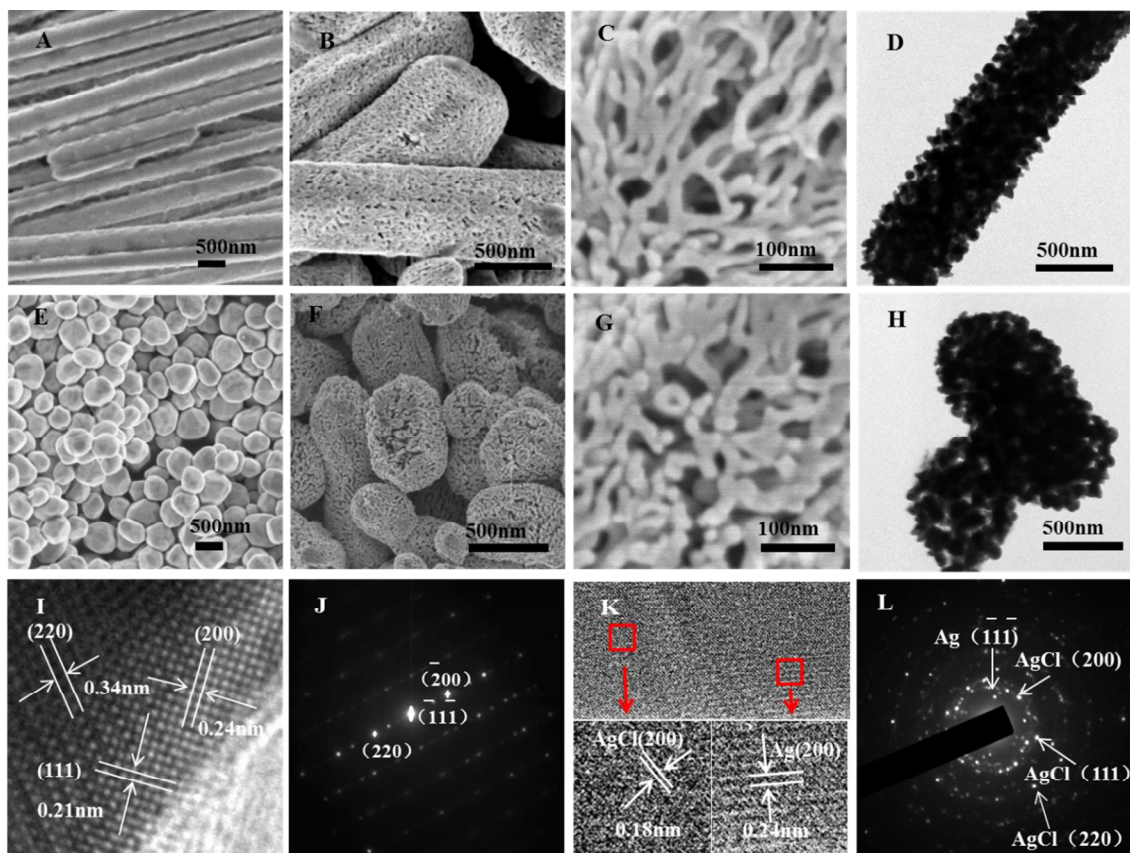


Fig. 2 SEM images of Ag NWs (A) and Ag nanospheres (E); SEM and magnification images of network-structured Ag/AgCl NWs (B, C) and nanospheres (F, G); TEM images of Ag/AgCl network-structured NWs (D) and nanospheres (H); HRTEM images and SAED patterns and of Ag NWs (I, J) and network-structured Ag/AgCl NWs (K, L).

Fig. 2 presents the FESEM and TEM characterization for Ag/AgCl network-nanostructures. The mean diameter of the sacrificial template Ag NWs is ~ 500 nm (Fig. 2A). As-synthesized 1D Ag/AgCl network-structures consist of the network NWs at the average diameter of ~ 20 nm and the pore channels at narrow macropore distribution from 50 nm to 100 nm (Fig. 2B and C). A distinct contrast of network NWs and pore channels can be observed clearly in TEM image in Fig. 1D, the dark is network Ag/AgCl NWs and the white interstices are pore channels. Similarly, the morphology of Ag/AgCl nano-networks fabrication from Ag nanospheres was shown in Fig. 2E-H. The average size of Ag/AgCl network-structured nanospheres and the Ag nanospheres are both ~ 500 nm. The diameters of the network NWs and the pore channel distribution are the same size as that of 1D Ag/AgCl network-structures fabricated from Ag NWs, which dues to the preparation under exactly the same condition except PVP. Fig. 2I shows typical HRTEM images of Ag NWs template. The fringe spacing of 0.21, 0.24 and 0.34 nm can be indexed to the (111), (220) and (220) planes, respectively, of face-centered cubic (fcc) Ag. The selected area electron diffraction (SAED) pattern from the same Ag NWs (Fig. 2J) exhibits a single crystal diffraction pattern with the indexed plane of ($\bar{1}\bar{1}\bar{1}$), (220) and ($\bar{2}\bar{0}\bar{0}$). The HRTEM image in Figure 2K shows the Ag/AgCl network-structures with the lattice spacing of 0.18 and 0.24 nm are corresponding to AgCl (200) and Ag (200) planes, respectively. The SAED pattern for Ag/AgCl network-structures illustrates clear crystalline spot ring (Fig. 2L), which corresponds to the polycrystalline structure with the indexed plane of AgCl (200), (111) and (220) and Ag ($\bar{1}\bar{1}\bar{1}$), indicating that the formation of Ag/AgCl network-structures.

Fig. 3 shows the typical XRD patterns of as-synthesized Ag NWs and Ag/AgCl network-structured NWs. Compared to that of pure Ag NWs, distinct diffraction peaks (2 θ) at 27.8°(111), 32.3° (200), 46.3° (220), 54.9° (311) and 57.5° (222) could be unambiguously detected. These diffraction peaks are attributed to the typical cubic phase of AgCl (JCPDS NO: 31-1238). At 38.1°, 44.4° and 64.2°, some diffraction peaks can also be found, which are consistent with the (111), (200) and (220) planes of Ag with face-centered cubic structure (JCPDS No: 01-1167). EDS analysis was adopted to determine the components of the network nanostructures. As shown in Fig. 3C, atomic ratio of Ag:Cl is approximately 7:3, which is much higher than the theoretic stoichiometric atomic ratio of 1:1 for Ag:Cl in AgCl. It indicates that the Ag elements of the higher part one exist in the form of elementary Ag, and the mole ratio between Ag and AgCl is approximately 4:3 in these network nanostructures. In order to clear understand the elemental distribution of the as-designed

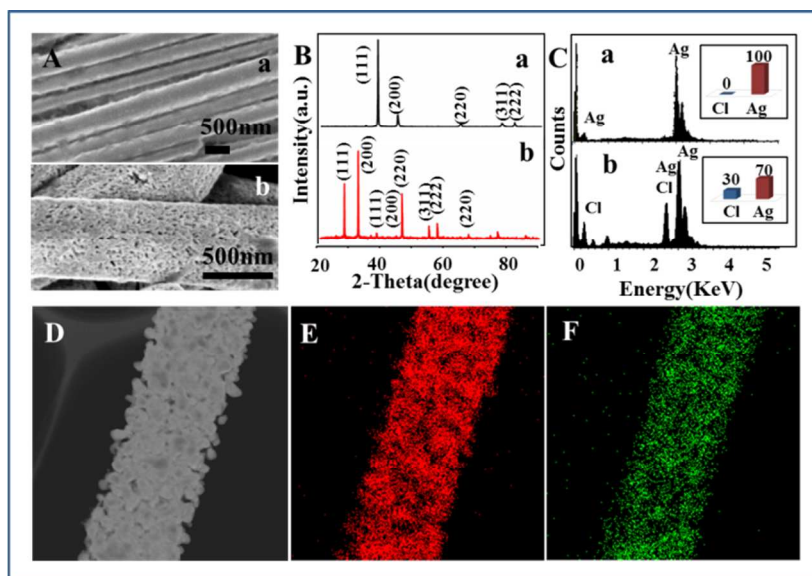


Fig. 3 SEM images (A), XRD patterns (B) and EDS analysis with inset of element accounts (C) of Ag NWs (a) and Ag/AgCl network-structured NWs (b); Elemental maps for Ag (E) and Cl (F) of a single sparse network-structured Ag/AgCl NW (D).

network structures, a single sparse Ag/AgCl network-structured NW is characterized by bright field scanning TEM (BF-STEM). Fig. 3D shows representative STEM image. Fig. 3E and F illustrate the corresponding EDS maps for Ag and Cl, in which the content of Ag is much higher than Cl, confirming the products are Ag/AgCl network-structured NWs.

The XPS spectra of Ag NWs and network-structured Ag/AgCl NWs samples are presented in Fig. 4, in which the numbers of emitted photoelectrons are given as a function of binding energy up to 800 eV. It can be observed that the Ag NWs present three photoemission peaks (Ag 3d, Cl 1s and O 1s)

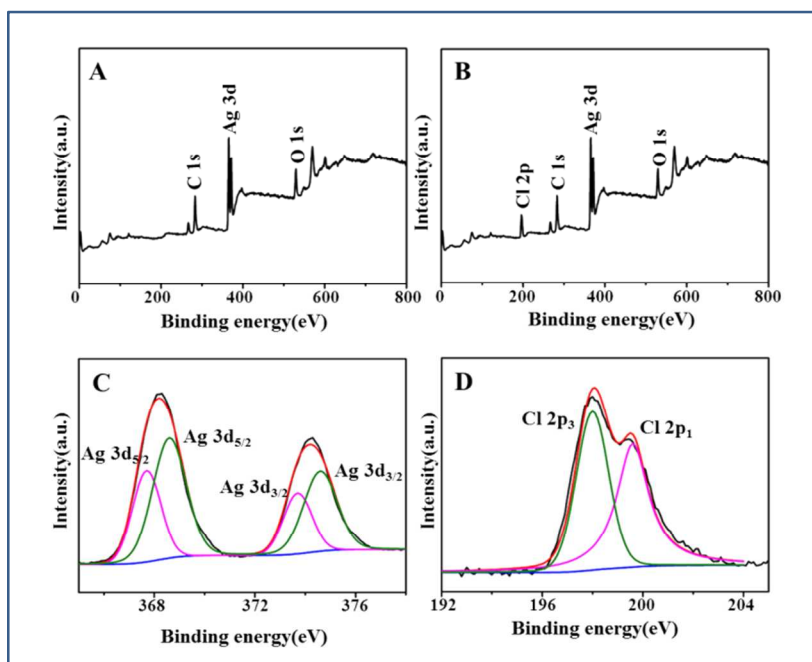


Fig. 4 XPS analysis of Ag NWs (A) and network-structured Ag/AgCl NWs (B) with the detailed spectra of Ag 3d (C) and Cl 2p (D).

in Fig. 4A. Meanwhile, another peak of Cl 2p appears in Ag/AgCl network-nanstructures in Fig. 4B. Magnified Ag 3d peaks in Fig. 4C, which consist of two sharp peaks 368.2 and 374.2 eV, which are owing to the spin-orbit splitting of 3d5/2 and 3d3/2, respectively. These peaks could be further separated into two peaks, respectively. 367.5, 368.4eV could be attributed to the Ag⁺ of AgCl, and 373.5, 374.4eV could be ascribed to Ag⁰. The semiquantitatively calculated surface mole ratio Ag:AgCl is approximately 4:3. These results matched well with the information of element analysis. For Cl, magnified Cl 2p peaks, which consist of two sharp peaks 199.6 and 198.0 eV, due to the spin-orbit splitting of 2p1 and 2p3, respectively (Fig. 4D).

The UV-vis diffuse reflectance spectra of as-prepared Ag/AgCl network-structured NWs and nanospheres as well as commercial P25-TiO₂ which was used as our reference photocatalyst are compared and shown in Fig. S4† in ESI. In contrast to P25-TiO₂ NPs, the Ag/AgCl network-structured nanocomposites have a strong absorption in visible region due to the plasmon resonance of Ag NPs in network nanostructures. The reason can be suggested that a wavelength of light is much greater than the diameter of Ag NP, the electromagnetic field across the entire Ag NP is essentially uniform. As the electromagnetic field oscillates, the weakly bound electrons of the Ag NP respond collectively, giving rise to a plasmon state. When the incident light frequency matches the plasmon oscillation frequency, light is absorbed, resulting in surface plasmon absorption. The NPs consisted in Ag/AgCl network structures have a large number of different shapes and diameters so that their plasmon oscillations cover a wide range of frequencies,^{33,34} and hence Ag/AgCl can absorb in a wide range of UV- and vis- light. Therefore, network Ag/AgCl nanostructures have excellent photocatalytic performance in visible light toward organic dyes, but as for chlorophenol, photodegradation under visible light is quite difficult to realize, even numbers of catalysts cannot do it under UV irradiation.

The photocatalytic performance and selectivity of as-synthesized catalysts were investigated in terms of the photodegradation of 4-CP under UV-light irradiation, and shown in Fig. 5. In order to exclude the possibility that the degradation of 4-CP was caused by the UV-light irradiation, the blank experiment was carried out where only 4-CP without any photocatalyst was involved (Fig. S5†). It can be proved that the irradiation does not degrade 4-CP in the absence of catalysts. To compare the photocatalytic performance of different catalysts, 4-CP was catalytic degradation by different catalysts, including Ag NWs, P25-TiO₂, network-structured Ag/AgCl NWs and nanospheres (Fig. 5A-B), and their UV spectra were illustrated in Fig. S6†. As shown in Fig. 5A, when Ag NWs are involved in the reaction system, the photodegradation of 4-CP can be negligible under UV irradiation. This can be suggested that the self-photo-sensitized decomposition of 4-CP under our experimental conditions could basically be ignored. While network-structured Ag/AgCl nanospheres and NWs were used as

photocatalysts, 90% and 80% degradation of 4-CP could be achieved, respectively, whose photocatalytic performance are much higher than that (5%) of commercially available P25-TiO₂. Compared with network-structured Ag/AgCl NWs, network-structured Ag/AgCl nanospheres display significant advantage, which owe much to the large surface areas and fertile active sites based on the same content of AgCl (Table S1†). As plotted in Fig. 5B, there is a nice linear correlation between ln(C/C₀) and the reaction time (t). It indicates that the photodecomposition reaction of 4-CP molecules photocatalyzed by our catalysts can be treated as a pseudo-first-order reaction. The rate constant (k) of the photocatalytic degradation of 4-CP over network-structured Ag/AgCl nanospheres is determined to be 0.28 min⁻¹, which is distinctly higher than that (0.10 min⁻¹) of network-structured Ag/AgCl NWs.

In addition, the selective-catalytic-degradation performances of network-structured Ag/AgCl nanospheres are evaluated toward the photodegradation of chlorophenol, including 2-CP, 3-CP and 4-CP. As shown in Fig. 5C, when network-structured Ag/AgCl nanospheres are involved in the reaction system, nearly 90% conversion can be achieved for 4-CP, while only about 30% and 10% conversions are given for 3-CP and 2-CP, respectively. It exhibits the selectivity of the catalysts of network-structured Ag/AgCl nanospheres which prefer to catalyse degradation of 4-CP. The reason is suggested to be caused by the steric hindrance which is an important factor for the catalytic reaction performance. The steric hindrance for three catalytic substrates decrease in the order: 2-CP > 3-CP > 4-CP, which is consistent with the order of photocatalytic activity. Therefore, steric hindrance can affect the absorption of catalysts to the catalytic substrates. Fig. 5D plots a nice linear correlation between ln(C/C₀) and the reaction time (t), and can be treated as a pseudo-first-order

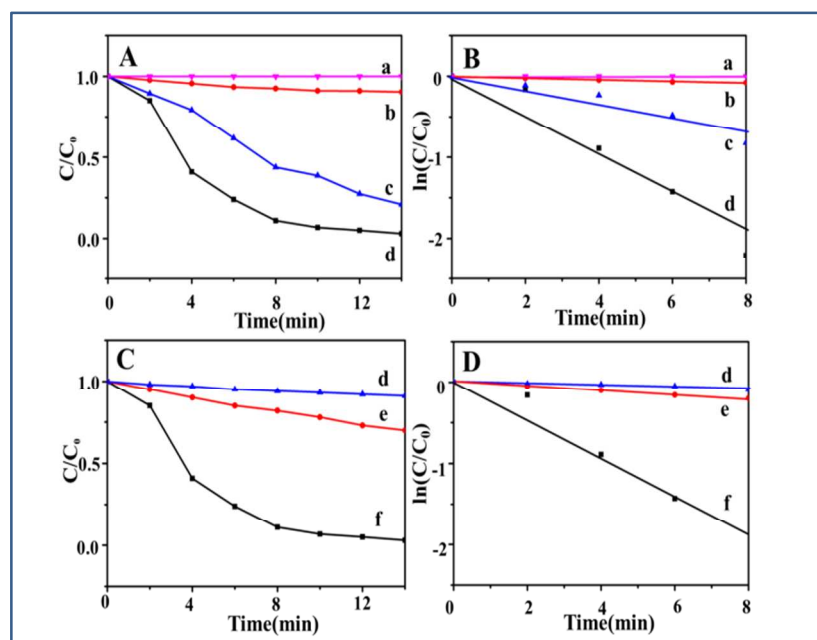


Fig. 5 (A, B) Plots of C/C_0 and $\ln(C/C_0)$ versus time for the photodegradation of 4-CP by Ag NWs (a), commercial P25-TiO₂ (b), network-structured Ag/AgCl NWs (c) and network-structured Ag/AgCl nanospheres (d); (C, D) Plots of C/C_0 and $\ln(C/C_0)$ versus time for the photodegradation of 2-CP (d), 3-CP (e) and 4-CP (f) by using network-structured Ag/AgCl nanospheres as catalysts under UV-light at r.t.

reaction. The rate constants (k) of the photocatalytic degradation of 2-CP and 3-CP over network-structured Ag/AgCl nanospheres are determined to be 0.011 min^{-1} and 0.025 min^{-1} , respectively.

As it is known, besides the catalytic activity, the recyclability of the catalysts is another principle substantially required by high-quality catalytic species. The stability of our network-structured Ag/AgCl plasmonic photocatalysts was also evaluated on the basis of performing the 4-CP degradation reactions repeatedly several times. As observed in Fig. 6, the catalysis performance decreased slightly after the sixth time. After the sixth catalysis routines, the morphology of catalysts still can be kept in completely, only a little structure collapse occurs in the catalytic process which can be seen in monitored SEM image (Fig. S7†). Thus, the as-designed network-structured Ag/AgCl nanocomposites have excellent stability in the catalytic degradation of 4-CP.

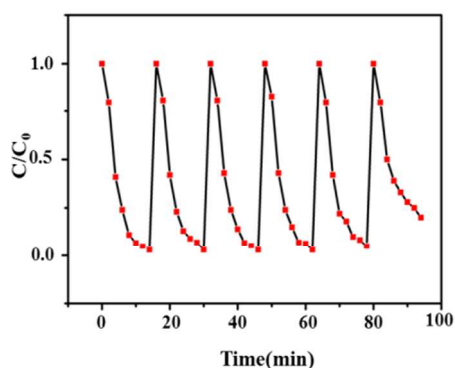


Fig. 6 Recyclability of photocatalytic degradation toward 4-CP catalyzed by network-structured Ag/AgCl nanospheres.

Conclusions

A special Ag/AgCl network-nanostructure was synthesized based on Ag NW or nanosphere templates through ELNC process. Offering large surface areas and lots of reaction performance chambers, the formulated Ag/AgCl network-nanostructures not only can provide firm frame support for the active sites, but also greatly facilitate reactant diffusion and transport. They could be used as high-performance yet durable UV-driven plasmonic photocatalysts for the selective-photodegradation of 4-CP. Compared with the commercially available P25-TiO₂ NPs, 3D Ag/AgCl network nanostructures could exhibit much higher photocatalytic performance, suggesting the good potential application for organic pollutant elimination.

Experimental

Chemicals

Copper(II) chloride dihydrate (CuCl₂·2H₂O, 99%), ethyl alcohol absolute (C₂H₅OH, 99%), Silver nitrate (AgNO₃, 99.8%), ethylene glycol (EG, 99%), Polyvinyl pyrrolidone (PVP, K30, Mw=58000; K90, Mw=800000) were all purchased from Sinopharm Chemical Reagent Co., Ltd.(SCRC). 2-chlorophenol (C₆H₅ClO, 99%), 3-chlorophenol (C₆H₅ClO, 98%) and 4-chlorophenol (C₆H₅ClO, 99%) were purchased from Alfa Aesar. P25-TiO₂ (ca.80% anatase and 20% rutile) nanospecies were purchased from Degussa and

used as the reference photocatalysts for comparison. All the reagents were used without further purification.

Preparation

The method was improved from that of Kan's group which used to obtain Ag NWs.³⁵ In a typical synthesis of 3D network-structured Ag/AgCl plasmonic photocatalysts, 0.204g AgNO₃, 0.204g CuCl₂·2H₂O and 0.1332g PVP (111 mg/mL, K90) were, respectively, dispersed in 10 mL of EG solution by sonication for 30 min, meanwhile, 10 mL EG solvent was magnetically stirred at 170 °C in a round-bottom flask. Then both AgNO₃ and PVP solutions were simultaneously injected drop-wise into the heated EG solution over a period of 5 min and kept for 80 min. And Ag NWs were obtained. Afterward, 10 mL 1.2×10⁻³ M CuCl₂ of EG solution was added to the mixture in drops in order to acquire network-structured Ag/AgCl NWs. The reaction stopped after 40 min when the mixtures turned to slightly purple. Magnetic stirring was applied throughout the entire process. After the system was cooled to room temperature, the resulting products were collected by centrifuge and washing with ethanol and deionized water in several times, followed the drying treatment under vacuum for further characterization. If PVP (K90) was taken place by PVP (K30), network-structured Ag/AgCl nanospheres can be acquired from Ag nanospheres.

Photocatalytic Test

In order to compare the photodegradation ability among the as-prepared Ag NWs, network-structured Ag/AgCl NWs, network-structured Ag/AgCl nanospheres and the commercial P25-TiO₂, the degradation of 4-CP (20 mg/L) solution is used to evaluate the photocatalytic activities of the prepared catalysts. The photocatalytic tests were performed in a reactor equipped with a cooling water-cycle system to keep the temperature stable. A 300 W mercury lamp was employed as the light source to produce UV irradiation. In a typical photocatalytic experiment, 30 mg Ag/AgCl were dispersed in 60 mL aqueous solution of 4-CP by sonication for 10 min, and the obtained suspension was magnetically stirred in the dark for 30 minutes to achieve adsorption-desorption equilibrium. During illumination, 2.0 mL suspension was withdrawn from the reactor every 2 minutes, followed by centrifugation and filtration, and the obtained clear solution was analyzed by ultraviolet spectroscopy. The concentration of 4-CP in the obtained sample was determined by detecting the absorption at 279 nm. In addition, to investigate the selective-catalytic-degradation performances of as-prepared network Ag/AgCl nanospheres, 2-CP, 3-CP and 4-CP photodegradation were also investigated under the same condition.

Characterization

The morphology and structure of the samples were investigated by FE-SEM (JEOL, S-4800, Japan), TEM and HRTEM (JEOL JEM-1200EX microscope, Japan). The elemental distribution and elemental mapping were carried out by STEM under the BF mode on a JEOL JEM-2100 F microscope. Element analysis was conducted by EDS conducted at 20 keV on a TN5400 EDS

instrument (Oxford). XRD patterns were recorded by using a Bruker D8 (German) diffractometer with a Cu K α radiation source ($\lambda=0.154056$ nm). XPS measurements were performed on a RBD-upgraded PHI-5000C ESCA system (Perkin Elmer) using Al K α radiation ($h\nu=1486.6$ eV). The whole XPS spectrum (0-800 eV) and the narrower, high-resolution spectra were all recorded using a RBD 147 interface (RBD Enterprises, USA). Binding energies were calibrated using the containment carbon (C1s=284.6 eV). UV-vis spectra of the samples were measured on an Agilent-8453 ultraviolet visible spectrophotometer. UV-vis diffuse reflectance spectra of the samples were obtained on an UV-vis spectrophotometer (Hitachi U-3010) using BaSO₄ as the reference.

Acknowledgements

This work is financial supported by National Natural Science Foundation (Nos: 21171130, 51271132, 51072134, and 91222103) and 973 Project (No: 2011CB932404) from China.

Notes and references

^aDepartment of Chemistry, Key Laboratory of Yangtze River Water Environment, Ministry of Education, Tongji University, 1239 Siping Road, Shanghai 200092, R. P. China.

^bShanghai Key Laboratory of D&A for Metal-Functional Materials, Tongji University, 4800 Caoan Road, Shanghai 201804, China.

E-mail: m_wen@tongji.edu.cn; Fax: (+) 86-21-65981097;

†Electronic Supplementary Information (ESI) available: Further details SEM images, XRD pattern, EDS data, UV-visible diffuse reflectance spectrum, and UV-vis absorption spectra of as-prepared catalysts for the degradation of 4-CP. See DOI: 10.1039/b000000x/

- 1 A. S. Cherevan, P. Gebhardt and C. J. Shearer, *Energy Environ. Sci.*, 2014, **7**, 791-796.
- 2 R. G. Li, H. X. Han and F. X. Zhang, *Energy Environ. Sci.*, 2014, **7**, 1369-1376.
- 3 C. Catrinescu, D. Arsene and C. Teodosiu, *Appl. Catal. B.*, 2011, **101**, 451-460.
- 4 O. Legrini, E. Oliveros and A. M. Braun, *Chem. Rev.*, 1993, **93**, 671-698.
- 5 H. Tada, T. Kiyonaga and S. Naya, *Chem. Soc. Rev.*, 2009, **38**, 1849-1858.
- 6 C. C. Chen, W. H. Ma and J. C. Zhao, *Chem. Soc. Rev.*, 2010, **39**, 4206-4219.
- 7 L. H. Wang, L. Xu, and Z. X. Sun, *RSC Adv.*, 2013, **3**, 21811-21816.
- 8 D. S. Bhatkhande, V. G. Pangarkar and A. A. C. M. Beenackers, *J. Chem. Technol. Biotechnol.*, 2002, **77**, 102-116.
- 9 M. R. Hoffmann, S. T. Martin and W. Choi, *Chem. Rev.*, 1995, **95**, 69-96.
- 10 A. Mills, R. H. Davies and D. Worsley, *Chem. Soc. Rev.*, 1993, **22**, 417-425.
- 11 D. Q. Zhang, G. S. Li and J. C. Yu, *J. Mater. Chem.*, 2010, **20**, 4529-4536.
- 12 X. B. Chen and S. S. Mao, *Chem. Rev.*, 2007, **107**, 2891-2959.
- 13 A. L. Linsebigler, G. Q. Lu and J. T. Yates, *Chem. Rev.*, 1995, **95**, 735-758.
- 14 A. Fujishima, T. N. Rao and D. A. Tryk, *J. Photochem. Photobiol. C: Photochem. Rev.*, 2000, **1**, 1-21.
- 15 C. Hu, Y. Q. Lan and J. H. Qu, *J. Phys. Chem. B*, 2006, **110**, 4066-4072.
- 16 H. L. Jiang and Q. Xu, *J. Mater. Chem.*, 2011, **21**, 13705-13725.
- 17 J. Song, J. Roh, I. Lee, *Dalton Trans.*, 2013, **42**, 13897-13904.
- 18 M. S. Zhu, P. L. Chen and W. H. Ma, *ACS Appl. Mater. Interfaces*, 2012, **4**, 6386-6392.
- 19 J. Y. Chen, B. J. Wiley and Y. N. Xia, *Langmuir*, 2007, **23**, 4120-4129.
- 20 B. Cheng, Y. Le and J. G. Yu, *J. Hazard. Mater.*, 2010, **177**, 971.
- 21 A. Murugadoss, N. Kai and H. Sakurai, *Nanoscale*, 2012, **4**, 1280-1282.
- 22 B. Erdem, R. A. Hunsicker and G. W. Simmons, *Langmuir*, 2001, **17**, 2664-2669.
- 23 Y. P. Bi, S. X. Ouyang and J. Y. Cao, *Phys. Chem. Chem. Phys.*, 2011, **13**, 10071-10075.
- 24 M. Ramstedt and P. Franklyn, *Surf. Interface Anal.*, 2010, **42**, 855-858.
- 25 C. H. An, S. Peng and Y. G. Sun, *Adv. Mater.*, 2010, **22**, 2570-2574.
- 26 E. Kazuma, T. Yamaguchi and N. Sakai, *Nanoscale*, 2011, **3**, 3641-3645.
- 27 P. Wang, B. B. Huang and X. Q. Qin, *Angew. Chem. Int. Ed.*, 2008, **47**, 7931
- 28 N. U. Silva, T. G. Nunes and M. S. Saraiva, *Appl. Catal. B*, 2012, **113-114**, 180-191.
- 29 Q. J. Xiang, J. G. Yu and B. Cheng, *Chem. Asian J.*, 2010, **5**, 1466-1474.
- 30 M. Wen, M. Z. Cheng and S. Q. Zhou, *J. Phys. Chem. C.*, 2012, **116**, 11702-11708.
- 31 B. L. Sun, M. Wen and Q. S. Wu, *Adv. Mater.* 2012, **10**, 2860-2866.
- 32 M. Z. Cheng, M. Wen and S. Q. Zhou, *Inorg. Chem.*, 2012, **51**, 1495-1500.
- 33 P. K. Jain, W. Y. Huang and M. A. El-Sayed, *Nano Lett.*, 2007, **7**, 2080-2088.
- 34 H. C. Guo, N. Liu and L. W. Fu, *Opt. Express*, 2007, **15**, 12095-12101.
- 35 C. X. Kan, J. J. Zhu and X. G. Zhu, *J. Phys. D: Appl. Phys.*, 2008, **41**, 155304-15531.